Appendix

De novo variants in LRRC8C resulting in constitutive channel activation cause a human multisystem disorder

Mathieu Quinodoz, Sonja Rutz, Virginie Peter, Livia Garavelli, Micheil A. Innes, Elena F. Lehmann, Stephan Kellenberger, Zhong Peng, Angelica Barone, Belinda Campos-Xavier, Sheila Unger, Carlo Rivolta, Raimund Dutzler, and Andrea Superti-Furga

Includes:

Appendix Clinical Reports

Appendix Figure S1-3

Table of Contents

Appendix Clinical Reports

P1, a boy, was born to healthy unrelated Italian parents who had two healthy daughters (Figure 1A). The pregnancy was unremarkable with normal foetal movements and karyotype. Delivery was by caesarean section at term with a birth weight of 2340g (3rd percentile), a length of 45cm (3rd percentile) and a head circumference of 31cm (2nd percentile, -2.1 SD). The APGAR score was 9 at both 1 and 5 minutes. Congenital anal atresia was noticed, and he was admitted to the Pediatric Surgical Department in Parma Hospital for surgery at age 3 days and then again at 11 months. At age 1 year, hypothyroidism was recognized and substitution therapy was begun. At age 4 years, anemia was diagnosed and he received monthly transfusions; Fanconi anemia was suspected but excluded by lab analysis (see below). Of note, he also had a marked telangiectasia with cutis marmorata from infancy, still persisting at age 17 years (Fig. 1).

He had dysmorphic signs with a small face, epicanthal folds, entropion and an upturned nose with bulbous tip. He had genua vara, slightly short thumbs, II-III and IV-V toe syndactyly on the right side and II-III toe syndactyly on the left side. At 2 years and 7 months, his length was 77.5cm (<1st percentile, -4.0 SD), his weight was 7740g (<1st percentile, -4.5 SD), his head circumference 42cm (<1st percentile, -4.6 SD) and pubertal stage A0 P1 S1 with 1ml testes bilaterally in the inguinal canal. Psychomotor development was delayed with sitting without support at 16 months, autonomous walking at 20 months, first words at 24 months.

He underwent extensive and repeated biochemical and metabolic investigations (TSH, FT3, FT4, thyroglobulin, Ab anti- thyroglobulin, Ab anti-TSH receptor, anti-peroxidase, coeliac markers, IGF1, IGFBP3, calcium, phosphorus, alkaline phosphatase, PTH and vitamin D 7-dehydrocholesterol, amino acids, organic acids, acylcarnitines) which were normal.

Throughout childhood, he had repeatedly reduced haemoglobin levels with measurements at 9.8, 10.7, 6.5 and 6.7 g/dl between 2 and 3.5 years and received transfusions. He was then hospitalized for severe anaemia (Hb 2.1g/dl) due to intestinal bleeding. Mean corpuscular volume was tested repeatedly and found to be between 70 and 77 fl, iron levels were also low, probably because of chronic GI bleeding. The diepoxybutane (DEB) test for Fanconi anemia was normal. Cell cycle analysis on T lymphocytes showed a percentage of cells incompatible with the diagnosis of Fanconi anemia. Morphological evaluation of a bone marrow smear showed rather scarce cells but with presence of all series and no atypical cells. A cytofluorimetric assessment on marrow blood showed moderate number of cells without evidence of maturing anomalies. Erythroid progenitor showed severely reduced clonogenic activity in the standard test but had a good response after the addition of the stem cell factor. Granulocyte-monocyte progenitor with clonogenic activity was absent. A bleomycin test and a test for sister chromatids exchange gave normal results. The hypothesis of Blackfan-Diamond anemia was considered (ADA activity was elevated at 3.37 U/g Hb – normal value 0.8-1.2 U/g Hb) but targeted sequencing of the genes *RPS19, RPL5, RPL11, RPS10*, *RPS26* did not reveal pathogenic variants. Sequencing of the genes *DKC1, TERC, TERT* and *TINF2* (exon 6 only) was also negative, making dyskeratosis congenita very unlikely. Finally, upper and lower GI tract endoscopy showed duodenal, ileal and colic micro-vascular telangiectasias and haemorrhagic fundus

gastropathy; a gastric biopsy was otherwise normal. A diagnosis of anemia because of chronic intestinal bleeding because of microvascular changes was retained.

Further genetic tests included karyotype (600 bands) and array-CGH (both normal). Targeted sequencing for variants in *SALL1* (for Townes-Brocks syndrome), *SALL4* (for Duane-radial ray syndrome) and *FAM58A* (for STAR syndrome), done because of the combination of syndactyly and anal atresia, was negative.
Echocardiography showed slight mitral prolapse PDA with left-right shunt and an abdominal ultrasound was normal. EEG showed temporal-parietal-occipital anomalies but a brain MRI was normal except for microcephaly. The ABR (auditory brainstem response) was also in normal range.
At the bone level, the X-Rays revealed a large anterior fontanel, thin frontal and parietal skull and wormian bones. X-Rays of the hands showed cup flaring of the distal radius and ulna, flaring of the distal 2nd, 3rd, 4th metacarpals and of the proximal phalanx of the 2nd, 3rd, 4th finger with a bone age of 9 months (Greulich and Pyle) at age 2 years and 3 months. Flaring of the metaphyses and cupping of the growth plate was seen at the distal femur and proximal tibia. The diaphyseal cortex of long bones was abnormally thin.
An ophthalmologic evaluation at 10 months revealed iris dystrophy with iris-lenticular synechiae, a pale retina with slightly pale optic disk suggestive of optic nerve atrophy, and inferior entropion. Re-evaluation at age 12 years showed severe bilateral visual impairment associated with several abnormalities including high myopia with elevated astigmatism, bilateral keratoconus, congenital entropion (operated), posterior iris synechia, strabismus (left eye esotropia), corneal changes with epithelial oedema and paracentral corneal leucoma, glaucoma with excavation of the papilla, pigmentary alterations of the fundus. He underwent glaucoma surgery. At the age of 16 he had a corneal transplant on the right eye.
At 12 years 2 months, his height was 112cm (<1st percentile, -5.1 SD), his weight 27kg (<1st percentile, -6.5 SD) and his head circumference 48.5cm (<1st percentile, -3.6 SD). The pubertal stages were A0 P1 B1 with 1ml testes bilaterally in the inguinal canal.
He showed osteopenia and had several fractures including that of the distal diaphysis of the femur, tibia and fibula, all after accidental trauma.

P2

The patient was the first-born child to her non-consanguineous parents of Canadian and Chilean origin. The pregnancy was complicated by intrauterine growth restriction detected in the third trimester. At 35 weeks of gestational age there was concern for fetal distress and she was delivered by emergency caesarian section. Birthweight was 1320 gm, OFC 26.5 cm and length 40 cm. However, APGAR scores were 8 at one minute and 9 and 5 minutes, and intensive resuscitation was not required. She was admitted to NICU for 18 days primarily for issues related to prematurity, feeding, small size and hypoglycemia. She was discharged home without any specific concerns regarding potential underlying genetic conditions or syndromes. In the subsequent month she was seen in the emergency department on one occasion owing to bloody stools. She was followed briefly in the neonatal follow-up clinic but discharged by two months of age. In follow-up as on outpatient she was found to have hyperammonemia and elevated lactate and was admittedly to investigate these findings at two and half months of age, which was the first involvement with

genetics and metabolic services. Over the course of this admission, she was noted to be small with relative microcephaly. Distinctive features including short upslanting palpebral fissures, cupped ears and 5th finger clinodactyly were noted. A karyotype and extensive metabolic testing, including a muscle biopsy suggestive of mild complex I deficiency, not confirmed on fibroblast testing were pursued with all other investigations being normal or non-diagnostic. She was initially discharged home on a modified low carbohydrate /high fat diet. The metabolic abnormalities subsequently disappeared and she was discharged from the metabolic service. She was followed by clinical genetics and several pediatric specialties throughout childhood. Several external consultations for additional opinions were pursued with no definitive diagnostic suggestions. Her growth eventually demonstrated some degree of catch up with persistent microcephaly. She was noted to have marked cutis marmorata telangiectatica congenita. Her problem list through childhood included global developmental delay (she was non-verbal), restricted mobility, and diagnoses of intellectual disability and spastic cerebral palsy. She had seizures with onset at 4 months of age, which had resolved and was maintained off anti-epileptic medications since age 15. She was G-tube fed, but able to tolerate oral feeding. She had a history of recurrent urinary tract infections and recurrent renal calculi. She had evidence of optic atrophy. Through adolescence she developed scoliosis. Prior investigations including normal array CGH (60k, 2011), normal DNA testing for Prader-Willi/Angelman (MS-MLPA), normal MECP2 sequencing and normal metabolic studies including TIEF, 7DHC, organic acids, purines profile, plasma amino acids, acylcarnitine profile, urine sulfites, MELAS and NARP point mutation sequencing and T-lymphocyte cultures for pyruvate carboxylase and propionyl-CoA-carboxylase deficiency. She had intermittent transient hypercalcemia and a history of hypercholesterolemia. An MRI at age 10 revealed microcephaly with T2/FLAIR signal within the periventricular white matter, particularly along the body of the lateral ventricle, subependymal cysts of the left lateral ventricle, and tiny periventricular cysts by the left frontal horn with evidence of volume loss with old gliotic changes in the left occipital lobe. These findings were similar to imaging pursued at age 4 years and suggestive of a prenatal ischemic injury. MRA did not reveal any abnormal vasculature. Skeletal radiographs showed gracile long bones, poorly developed glenoid fossa, slender ribs and overtubulated long bones with metaphyseal irregularities. At age 15 she developed acute idiopathic hypertension, with systolic blood pressure exceeding 200. She was placed on amlodipine, which not only was successful in managing the hypertension, but also resulted in a striking improvement of her until then long-standing underlying cutis marmorata. She was reassessed at age 19 by Clinical Genetics, at the request of the family to determine suitability for clinical whole exome sequencing. Despite her extensive medical problem list and cognitive differences, she was thriving in the community. There was no evidence of regression, and indeed she continued to make developmental gains. She was active in various activities, and enjoyed being out in the community, for example biking on her modified bicycle with her dog for hours per day. She was clinically stable but had developed autoimmune liver disease after an EBV infection. She was noted to have deep set eyes, hypotelorism, a short and upturned nose. There was no residual evidence of cutis marmorata. She was engaged and friendly and could communicate in short phrases. While her features were distinctive, no specific clinical diagnosis came to mind. She remained the only biological child of her parents and the family history was otherwise non-contributory. While the testing was underway, she was admitted to hospital at age 20 in the context of an

acute influenza A infection. She presented in acute respiratory failure and developed gastric necrosis that was not amenable to surgery. She died three days after admission.

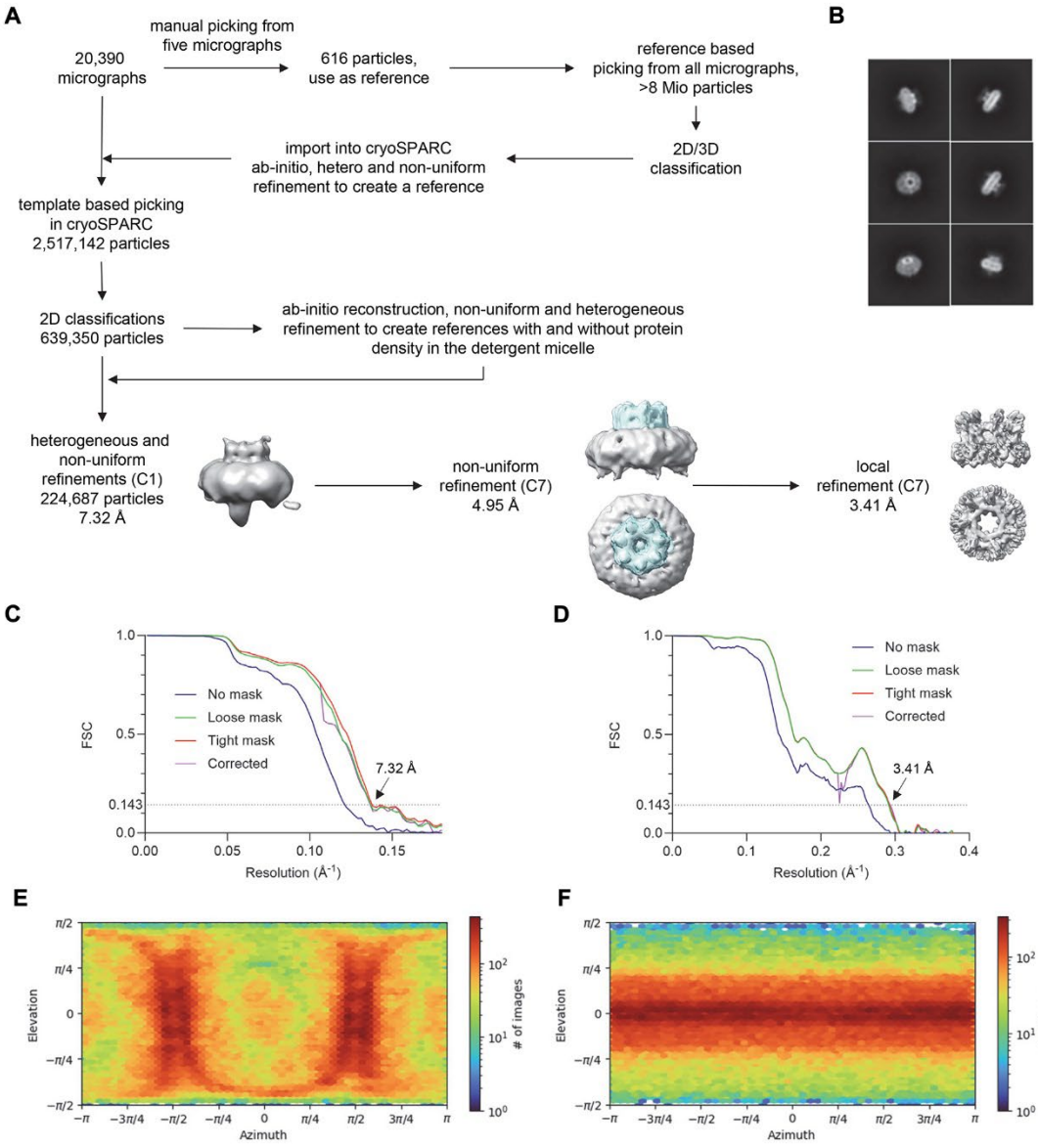

Appendix Figure S1. Cryo-EM structure of hLRRC8C^{trunc}.

A. Data processing workflow. Particles were manually picked from five micrographs in Relion (Zivanov *et al*, 2018) and used for reference-based particle picking from all micrographs. Particles were subsequently subjected to 2D and 3D classifications and, in case they contained protein density, they were imported into cryoSPARC (Punjani *et al*, 2017). Following ab-initio reconstruction and hetero- and homogeneous refinement steps, an improved reference map was generated that was used for template-based particle picking from all micrographs in cryoSPARC. The picked particles were cleaned up by 2D classification. Reference volumes with and without protein density in the detergent micelle were created using ab-initio reconstructions, non-uniform and heterogeneous refinement. These references were used for several

rounds of heterogeneous and non-uniform refinement with all particles selected after 2D classification, leading to a map with a resolution of 7.32 Å (with C1 symmetry). The non-uniform refinement was repeated with C7 symmetry applied, leading to an improvement of the resolution to 4.95 Å. A subsequent local refinement step with a mask surrounding the ESD region (blue), improved the resolution to 3.41 Å.

B. Representative 2D class averages of the LRRC8C^{trunc} channel.

C, D. FSC plots of the cryo-EM density maps refined with C1 symmetry (C) and of the locally refined ESD with C7 symmetry applied (D). The dotted line indicates the resolution at which the FSC drops below the 0.143 threshold.

E, F. Heatmaps displaying the angular distribution of particle orientations for the model refined with C1 symmetry (E) and for the final model after local refinement with C7 symmetry (F).

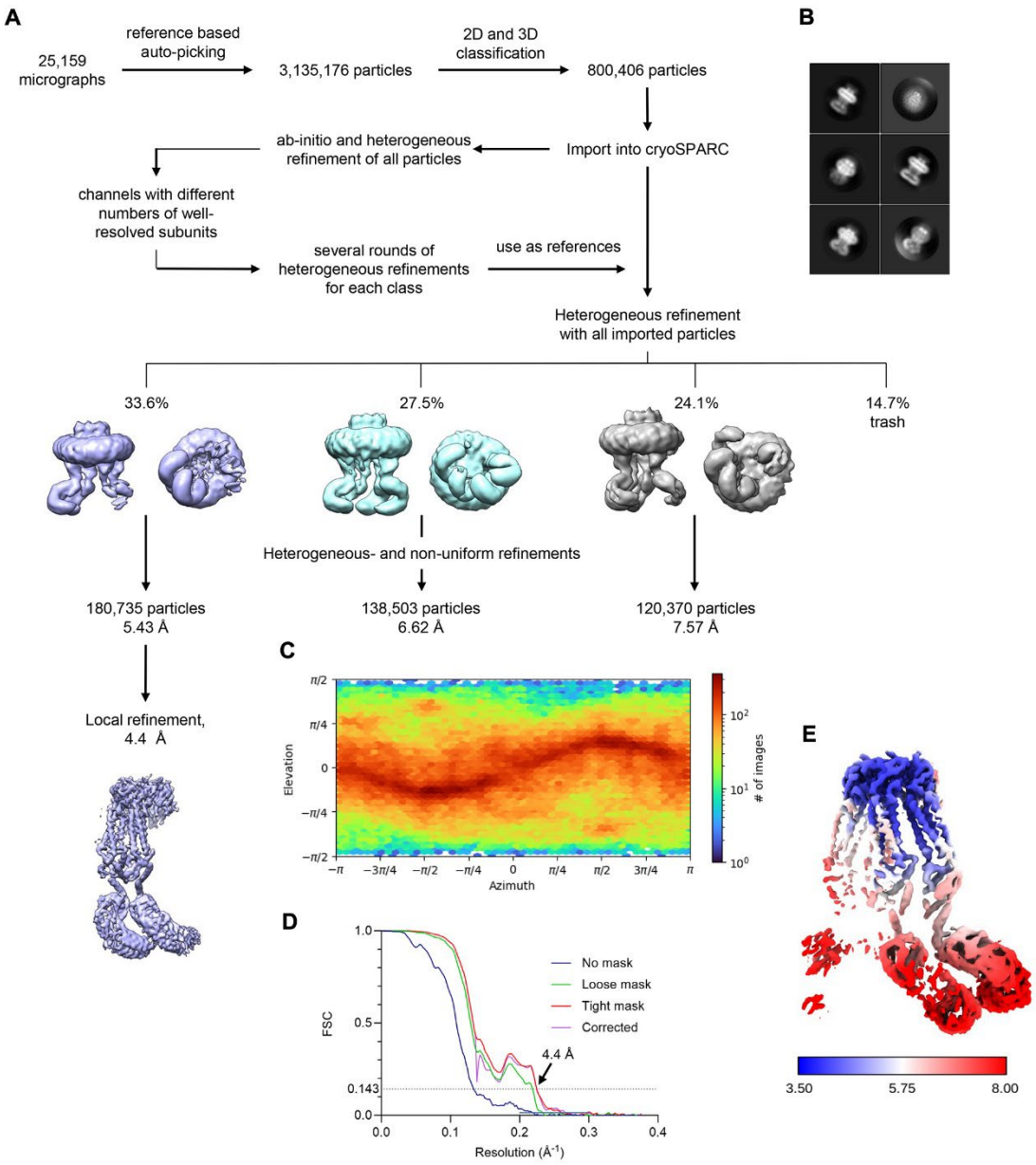

Appendix Figure S2. Cryo-EM structure of hLRRC8C^{V390L}.

A. Data processing workflow. Particles were sorted during 2D and 3D classification in Relion and selected class averages showing protein features were imported into cryoSPARC. Particles were initially applied to ab-initio reconstruction and heterogeneous refinement. Classes with different numbers of defined subunits were improved in several rounds of heterogeneous refinement resulting in maps showing two, three or four well-defined subunits. These maps were used as references for a heterogeneous refinement step with all originally imported particles. The distribution of particles (%) is indicated. Heterogeneous and non-uniform refinement has led to final maps containing different numbers of well-resolved subunits. For the map reaching the highest resolution, a local refinement step was performed with a mask around protein density

at a contour where the detergent micelle was not resolved. The best resolved map (at 4.4 Å) was used for the comparison with hLRRC8C^{WT}.

B. Representative 2D class averages of the hLRRC8C^{V390L} homomer.

C. Heatmap displaying the angular distribution of particle orientations.

D. FSC plot of the final cryo-EM density map used for the estimation of its resolution. The dotted line indicates the resolution at which the FSC drops below the 0.143 threshold.

E. Final 3D reconstruction colored according to local resolution.

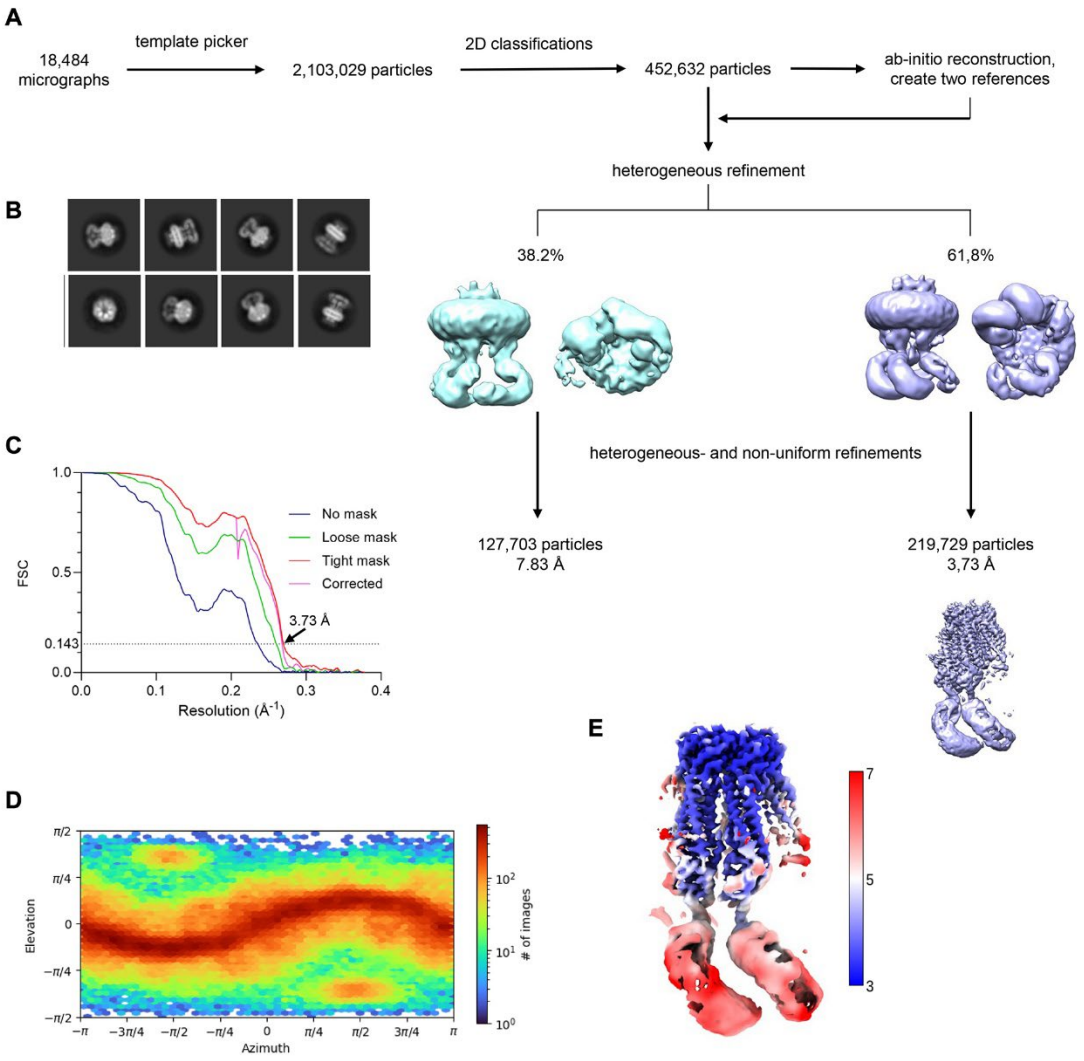

Appendix Figure S3. Cryo-EM structure of hLRRC8C^{WT}.

A. Data processing workflow. Particles were picked in cryoSPARC and cleaned-up during 2D classifications. An ab-initio reconstruction resulted in two maps that were used as references in a heterogenous refinement step with all particles selected after 2D classifications. The distribution of particles (%) is indicated. With further heterogenous and non-uniform refinement steps of the two resulting classes, maps were generated with different numbers of well-resolved subunits. The map reaching the highest resolution was used for the comparison with the hLRRC8C^{V390L} map and is shown.

B. Representative 2D class averages of the LRRC8C^{WT} channel.

C. FSC plot of the final cryo-EM density map used for the estimation of its resolution. The dotted line indicates the resolution at which the FSC drops below the 0.143 threshold.

D. Heatmap displaying the angular distribution of particle orientations.

E. Final 3D reconstruction colored according to local resolution.

References

Punjani A, Rubinstein JL, Fleet DJ, Brubaker MA (2017) cryoSPARC: algorithms for rapid unsupervised cryo-EM structure determination. *Nat Methods* 14: 290-296

Zivanov J, Nakane T, Forsberg BO, Kimanius D, Hagen WJ, Lindahl E, Scheres SH (2018) New tools for automated high-resolution cryo-EM structure determination in RELION-3. *Elife* 7